Green Chemistry

A nano tetraimine Pd(0) complex: synthesis, characterization, computational studies and catalytic applications in the Heck–Mizoroki reaction in water†

Zeinab Mandegani, Mozaffar Asadi,* Zahra Asadi, Afshan Mohajeri, Nasser Iranpoor and Akbar Omidvar

A new nano tetraimine Pd(0) complex was successfully prepared by the complexation of palladium acetate with an *N,N*-bisimine ligand. The structural features of the catalyst and the ligand were characterized using different microscopic and spectroscopic techniques such as FT-IR, XRD, XPS, UV–Vis, NMR, and elemental analysis. The morphology of the catalyst was determined using FE-SEM and TEM. The catalyst was effectively employed in the palladium-catalyzed Heck–Mizoroki reaction in water as a green solvent. The catalyst was reusable and recycled six times without any decrease in its catalytic activity. The ICP analysis showed that the catalyst has very little Pd leaching (0.2%) during the reaction process, demonstrating that our catalyst is stable and heterogeneous in practice. Furthermore, we have theoretically explored the feasibility of two neutral and cationic pathways in the density functional theory framework. The geometries and energies of all species involved in the reaction mechanism are analyzed.

Introduction

Palladium-mediated Heck–Mizoroki coupling reactions have received considerable attention due to the industrial applications of these reactions in fine chemical fields, such as pharmaceuticals and herbicides.[1] These reactions generally proceed in the presence of a homogeneous palladium catalyst which has two main drawbacks, a tedious work-up and recovery process and palladium contamination in products.[2] One way of overcoming these difficulties would be the use of heterogeneous catalyst systems instead of homogeneous counterparts for application in industrial reaction processes. Along this line, many heterogeneous palladium catalysts have been developed for the cross-coupling reactions, especially in the Heck–Mizoroki coupling reaction.[3–6] On the other hand, one of the most widely used types of ligands in the homogeneous palladium-catalyzed Heck reactions is phosphine ligands. However, phosphine ligands used in these reactions are sensitive to air oxidation and thus often require air-free conditions, which poses significant inconvenience in their synthetic appli-

cations.[7] Some of these ligands are comparatively difficult to make or rather are more expensive and often lead to competitive degradation of the Pd catalyst through the P–C bond cleavage of a coordinated phosphine ligand.[8] Also, there is a strong tendency to avoid the application of these ligands because of their possibly negative impact on the natural environment.[9] As a result, in recent years, extensive effort has been dedicated to exploring the effective phosphine-free Pd complexes bearing N-heterocyclic carbene ligands,[10] bispyrazole derivatives,[11,12] bispyridine,[13] bisimidazole,[14,15] bisbenzoimidazole,[16] N_2-donor ligands,[17,18] or even N_4-tetradentate[19] as alternative ligands. Among the phosphine-free catalysts, a key feature is the stabilization of the active catalysts, which depends on the ligand stability, chelation or steric shielding of the metal center and the strength of the metal–ligand bond.[20] Therefore, in recent years, transition-metal complexes containing N-donor ligands have received much attention and have shown that ligands strongly donate electrons to the metal center, thus stabilizing various oxidation states of metals.[20,21] The concept of green chemistry has been defined as the design of chemical products and processes to reduce or eliminate the use and generation of hazardous solvents and was developed in principle to guide the chemists in their search for greenness.[22,23] Water, as a non-toxic, plentiful, and non-flammable solvent, has a high heat capacity and is relatively inexpensive.[24,25] Consequently, in the context of green

*Department of Chemistry, College of Sciences, Shiraz University, Shiraz 71454, Iran.
E-mail: asadi@susc.ac.ir; Fax: +98 713 646 0788; Tel: +98 713 613 7121*

chemistry, heterogeneous catalysis of reactions carried out under aqueous conditions is considered environmentally friendly, since water could be considered as the safest solvent.[26]

Since sustainable development involves the utilization of reusable catalysts, the search for new catalytic systems to replace existing homogeneous ones is one important issue. Therefore, in this study, in continuation of a previous study in the field of coordination chemistry we would like to introduce the use of a nano tetraimine Pd(0) complex without added phosphine ligands in the Heck–Mizoroki reaction in water under mild and environmentally benign conditions. The Heck reaction has also been the subject of many theoretical studies[27–30] and different kinds of ligands have been considered. However, the complex nature of the reaction still leaves many questions unanswered, such as the superiority of neutral and cationic pathways under conditions where both could be possible. Accordingly, in the Theoretical calculations section of the present paper, we have investigated the model reaction for both cationic and neutral versions of the Heck reaction.

Experimental

General

All chemicals were purchased and were used without any further purification. The progress of the reactions was followed by TLC using silica gel polygrams SIL G/UV 254 plates or by GC using a Shimadzu gas chromatograph GC-14A equipped with a flame ionization detector and a 3-meter length glass column packed with DC-200 stationary phase and nitrogen as the carrier gas. Fourier transform infrared spectroscopy (FT-IR) analysis of the samples was performed on a Shimadzu FT-IR 8300 spectrophotometer, and the sample and KBr were pressed to form a tablet. The ^{1}H NMR and ^{13}C NMR spectra were recorded on a Bruker Avance DPX 250 MHz spectrometer in CDCl$_3$ or DMSO-d$_6$ solvents using TMS as an internal standard. X-ray powder diffraction (XRD) spectra were recorded on a Bruker AXS D8-Advance X-ray diffractometer with CuKα radiation (λ = 1.5418). X-ray photoelectron spectroscopy (XPS) measurements were conducted with an XR3E2 (VG Microtech) twin anode X-ray source using AlKα = 1486.6 eV. Transmission electron microscopy (TEM) images were obtained on a Philips EM208 transmission electron microscope with an accelerating voltage of 100 kV, and field emission scanning electron microscopy (FE-SEM) images were obtained on a HITACHI S-4160. UV spectra (PerkinElmer, Lambda 25, UV–Vis spectrometer) were used to ensure complete conversion of Pd(II) to Pd(0). Mass spectra were obtained at 70 eV. The amount of palladium nanoparticles supported on the N,N-bisimine ligand was measured using an ICP analyzer (Varian, Vista-pro) and atomic absorption spectroscopy. All yields refer to the isolated products. Elemental analyses were done on a 2400 series Perkin-Elmer analyzer. Melting points were determined with a Buchi 510 instrument in open capillary tubes and are uncorrected.

All products were identified by comparison of their spectral data and physical properties with those of authentic samples, and all yields refer to the isolated products.

Procedure for the preparation of the N,N-bisimine ligand (3)

To the solution of ethylene diamine (2.0 mmol, 0.13 mL) in 10 mL ethanol was added dropwise a stoichiometric amount of 4-chloro benzaldehyde (4.0 mmol, 0.56 g). A white solution, which was obtained due to the imine formation, was stirred at room temperature for 10 h. The resulting N,N-bisimine ligand, as a white precipitate, was separated by filtration and washed with ethanol (2 × 5 mL) and then dried in a vacuum. The crude product was recrystallized from ethanol to obtain the pure product. FT-IR (KBr pellets, cm^{-1}): 2839–3062 (CH stretching), 1643 (C=N), 1480–1600 (C=C), 1473 (CH$_2$ bending), 1167 (C–N), 748 (C–Cl). ^{1}H NMR (250 MHz, CDCl$_3$): (ppm) 3.95 (s, 4H, CH$_2$); 7.34 (d, 4H, CH aromatic, J = 7.5 Hz); 7.60 (d, 4H, CH aromatic, J = 7.5 Hz); 8.22 (s, 2H, CH). ^{13}C-NMR (63 MHz, CDCl$_3$): δ (ppm) 61.4, 128.8, 129.2, 134.5, 136.6. Anal. Calc. for C$_{16}$H$_{14}$N$_2$Cl$_2$ (%): C; 62.97; H, 4.59; N, 9.18. Found (%): C, 62.04; H, 4.41; N, 9.07.

General procedure for preparation of the nano tetraimine Pd(0) complex (4)

To prepare the nano tetraimine Pd(0) complex, to a solution of the N,N-bisimine ligand (2.0 mmol, 0.61 g) in ethanol (10 mL) under an N$_2$ atmosphere was added Pd(OAc)$_2$ (1.0 mmol, 0.22 g) and the mixture was refluxed for 3 h until the reaction was completed. After the completion of complex formation, the solvent was removed by filtration, and the resulting solid was washed with hot ethanol (3 × 2 mL) and water (3 × 2 mL) and dried at 80 °C overnight. Yield: 92.7% (0.64 g). FT-IR (KBr pellets, cm^{-1}): 2839–3062 (CH stretching), 1597 (C=N), 1480–1600 (C=C), 1473 (CH$_2$ bending), 1152 (C–N), 751 (C–Cl), 467 (Pd–N). Anal. Calc. for C$_{32}$H$_{28}$Cl$_4$N$_4$Pd (%): C; 59.51; H, 4.37; N, 8.67. Found (%): C, 59.00 H, 4.30; N, 8.80.

General procedure for the Heck–Mizoroki reaction using the nano tetraimine Pd(0) complex as the catalyst

Aryl halide (1.0 mmol) and alkene (1.2 mmol) were added to a flask containing Pd(0) complex nanoparticles (0.005 g of the catalyst, containing 0.004 mmol of palladium) and K$_2$CO$_3$ (2.0 mmol) in the presence of water (3 mL). The flask was placed in an oil bath at 90 °C for the appropriate time (Table 2). GC and TLC analyses of the reaction mixture showed the completion of the reaction. After consumption of the starting material, the resulting hot reaction mixture was filtered quickly through a thick cellulose filter paper under diminished pressure and washed with diethyl ether (2 × 5 mL). The organic phase was separated and dried over anhydrous Na$_2$SO$_4$ and evaporated. The resulting crude product was purified by flash chromatography to give the desired pure product in high to excellent isolated yields.

Typical procedure for the Heck–Mizoroki reaction and recycling of the catalyst

Iodobenzene (1.0 mmol, 0.1 mL) as a model compound was reacted with *n*-butyl acrylate (1.2 mmol, 0.18 mL) in the presence of 0.4 mol% of the Pd catalyst (5 mg) and K_2CO_3 (2 mmol, 276.4 mg) at 90 °C in water (3 ml). After completion of the reaction and cooling the mixture to room temperature, diethyl ether (2 × 5 mL) was added to the reaction mixture. The organic phase was separated from the aqueous layer by using a syringe and the coupled product was isolated by chromatography on a short column of silica gel using *n*-hexane/ethyl acetate as the eluent. The coupled product was obtained in 94% yield (187 mg). The aqueous phase containing the catalyst was centrifuged. Removal of the aqueous layer by decantation or by using a syringe left the solid catalyst, which was washed with diethyl ether (3 × 2 mL) again in order to remove any remaining organic compound. The catalyst was dried in a vacuum oven and was used again for the next run.

Large scale reaction for the Heck–Mizoroki reaction of iodobenzene with *n*-butyl acrylate

A large scale reaction was performed using iodobenzene (10 mmol, 1.0 mL), *n*-butyl acrylate (12 mmol, 1.8 mL), 4.0 mol% (0.05 g) of the Pd catalyst and K_2CO_3 (20 mmol, 2.7 g) in distilled water (20 mL) at 90 °C. Work-up of the reaction mixture was performed as in the above procedure. The desired coupled product was obtained in 90% yield (1.78 g). The catalyst was also separated as above and reused for the next run.

Results and discussion

Catalyst preparation and characterization

The synthetic route for the preparation of the catalyst is shown in Scheme 1.

The nano tetraimine Pd(0) complex (**4'**) was obtained which was characterized using different microscopic and spectroscopic techniques including FT-IR, XRD, XPS, UV–Vis, and elemental analysis.

Fig. 1 shows the FT-IR spectra of the pure *N,N*-bisimine ligand and its nano tetraimine Pd(0) complex. The *N,N*-bis-
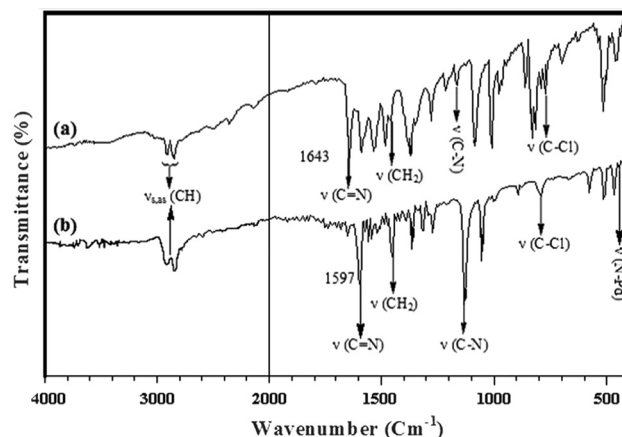

Fig. 1 FTIR spectra of (a) *N,N*-bisimine ligand and (b) the nano tetraimine Pd(0) complex.

imine ligand exhibited a band at 1643 cm^{-1} due to the azomethine $\nu(C{=}N)$ stretch (Fig. 1). This band appears at low frequency of shift of 1597 cm^{-1} in the spectrum of the complex, indicating the coordination of azomethine nitrogen to the palladium ion.[31] In the lower frequency region, a band appears at 467 cm^{-1} due to $\nu(Pd–N)$ vibration in the nano tetraimine Pd(0) complex.

These vibrational bands at 1597 and 467 cm^{-1} confirm the successful coordination of the nitrogen atoms with the palladium(0) by covalent interaction. Vibrations in the range of 1480–1600 cm^{-1} are attributed to the aromatic ring. Also, Fig. 1b shows the FT-IR spectrum of the nano tetraimine Pd(0) complex catalyst; the bands at 751, 1152, 1473 and 1400–1480 cm^{-1} are attributed to C–Cl (stretching vibration), C–N (stretching vibration) and N–H (bending), and CH_2 (bending), C=C (aromatic ring stretching), respectively. Also, the presence of several bands with medium intensity in the 2839–3062 cm^{-1} region is allocated to C–H stretching of groups (symmetric and asymmetric stretching).

The powder X-ray diffraction (XRD) pattern for the catalyst showed the expected crystallinity of Pd(0) nanoparticles (Fig. 2).
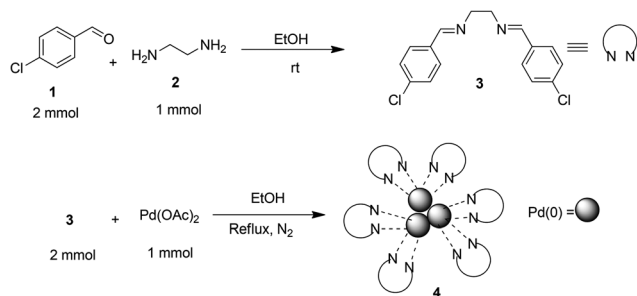
Scheme 1 The route for the synthesis of the nano tetraimine Pd(0) complex.
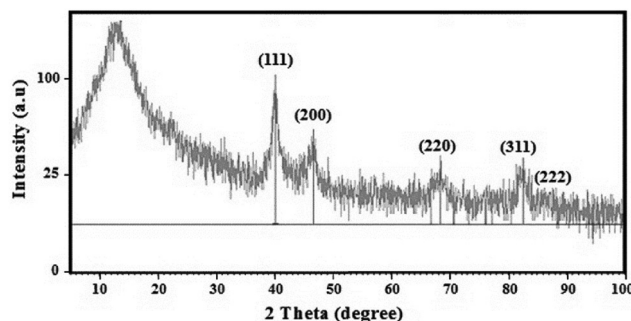

Fig. 2 XRD patterns of the nano tetraimine Pd(0) complex.

Fig. 2 shows broad peaks of 2θ values 40.1, 46.6, 68.1, 82.2 and 86.5 degrees, which are assigned to the corresponding (111), (200), (220), (311) and (222) indices of the face centered cubic (fcc) lattice of metallic Pd.[32] The Pd nanoparticle size was estimated, using the by Scherrer equation from XRD pattern data, to be 9 nm. $D = 0.9\lambda/\beta\cos\theta$, where D is the average diameter in Å, λ is the wavelength of the X-rays, β is the broadening of the diffraction line measured at half its maximum intensity in radians and θ is the Bragg diffraction angle. The calculated size matches approximately the size observed from TEM images. The same result was also obtained for the XRD pattern of the catalyst after its use in the Heck–Mizoroki reaction for several cycles. This reveals the excellent stability of the catalyst after recycling.

In order to have more information about the chemical structure of this complex, the mole ratio technique was employed.[33] The obtained spectrophotometric data showed that the structure of the complex should be ML_2, which is in consistent with the obtained elemental analysis.

The FE-SEM and TEM images of the prepared nano tetraimine Pd(0) complex are shown in Fig. 3.

The morphology and size of Pd(0) nano particles were studied by FE-SEM (Fig. 3a). It seems that the particles are semispherical in the FE-SEM image (Fig. 3a) with some agglomerations of the particles. Fig. 3b and c show the properties of the catalyst before and after six cycles in the Heck–Mizoroki reaction of iodobenzene as the model reaction. Transmission electron microscopy (TEM) images of the Pd nanosphere in both samples appear almost unchanged in their size and shape. These images show that the average size of the Pd nano particles entrapped by the N,N-bisimine ligand is around 10 nm.

According to the information which was obtained from the microscopic and spectroscopic techniques, the chemical structure of the catalyst was proposed as shown in Scheme 2. It seems that the generated Pd nanoparticles are stabilized by an organic layer that originated from the tetraimine ligand. These nanoparticles could well be stabilized by the ligand via the interaction of Pd(0) with the iminum nitrogen atoms.

The amount of palladium content of the catalyst was determined by induced coupled plasma (ICP) analysis and atomic absorption spectroscopy (AAS). According to the ICP and AAS results the amount of palladium was found to be 0.78 mmol per gram of the complex.

The resulting Pd supported nanoparticles were also characterized by UV–Vis spectroscopy to ascertain the conversion of Pd(II) to Pd(0). This was supported by the disappearance of the peak at around 420 nm (Fig. 4a).

Then, XPS was utilized as a useful tool to study not only the coordination of the ligand and palladium but also the chemical state of palladium present in the catalyst. Fig. 4b shows the fully scanned spectrum in the range of 0–1200 eV. The peaks at 181.9, 290.8, 344.6 and 404.6 eV are attributed to Cl, C, Pd and N atoms, respectively. The X-ray photoelectron spectrum of the nano tetraimine Pd(0) complex exhibits peaks at 335.7 and 340.8 eV that are assigned to $3d_{5/2}$ and $3d_{3/2}$ of palladium
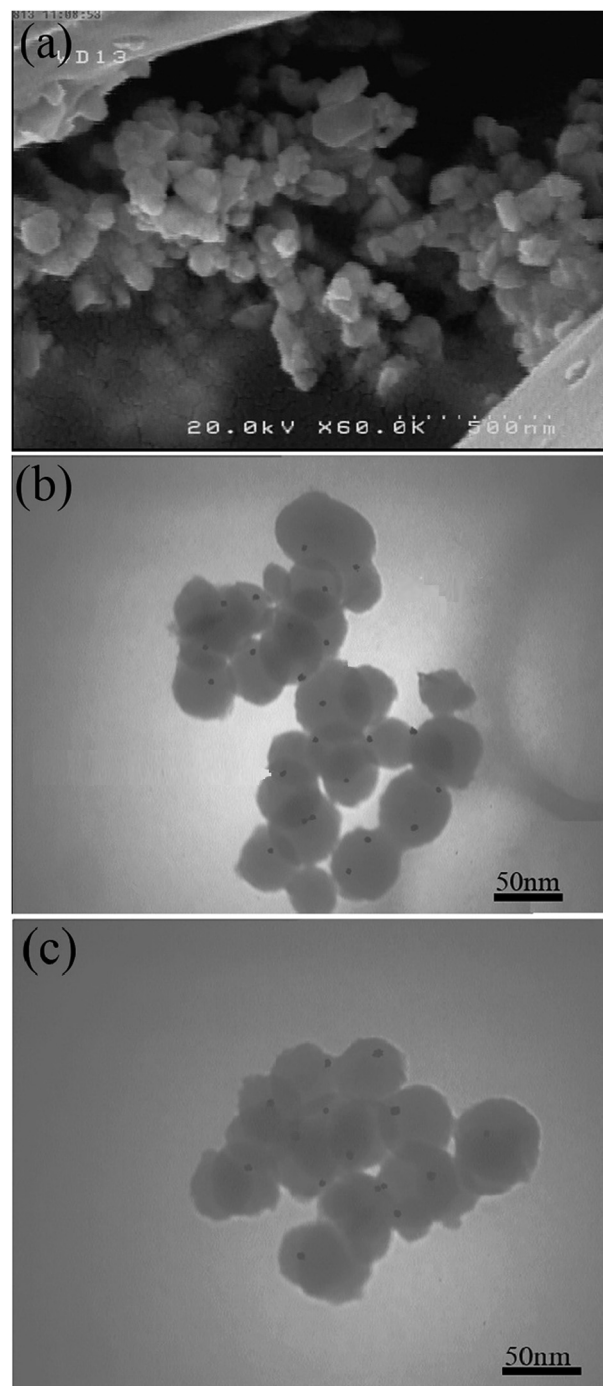

Fig. 3 FE-SEM image of the Pd(0) particles (a) and TEM pictures of the Pd(0) particles before using in the reaction (b) and after recycling in the 6th run (c) used for the reaction of iodobenzene with n-butyl acrylate.

in the zero oxidation state, respectively (inset) (Fig. 4b).[34] This absorption doublet typically seen in Pd^0 containing catalysts confirms that most of the Pd^{2+} ions have been reduced to Pd^0. However, we found that the Pd $3d_{5/2}$ and $3d_{3/2}$ peaks shifted to higher values as a result of the presence of the nitrogen groups of the N,N-bisimine ligand. It is also well recognized
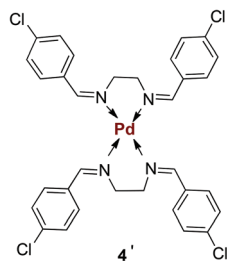
Scheme 2 The structure of the nano Pd(0) complex obtained by the mole ratio method.
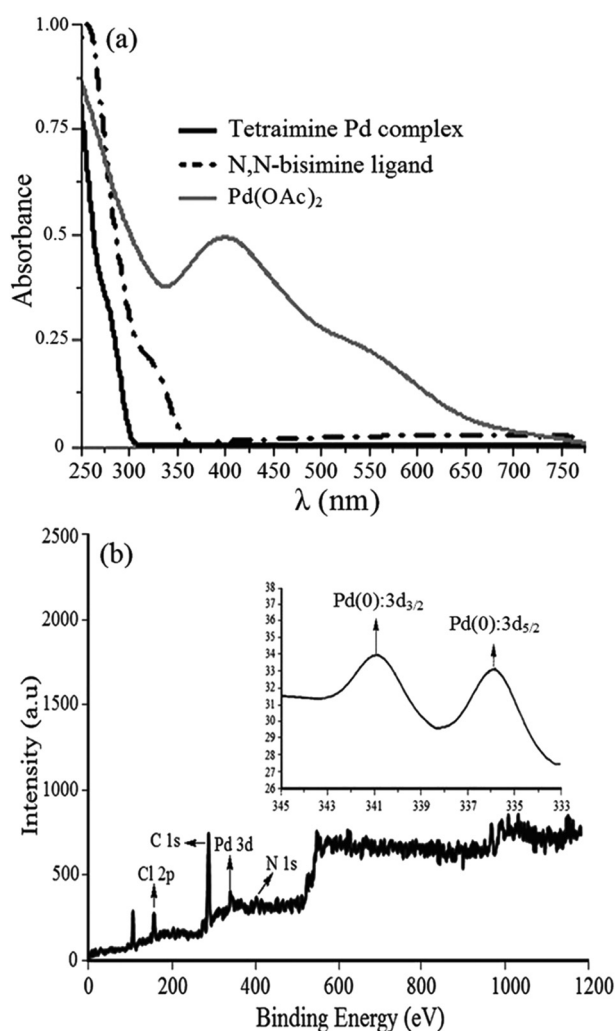
Fig. 4 (a) UV−Vis spectra of Pd(OAc)$_2$, N,N-bisimine ligand and the nano tetraimine Pd(0) complex. (b) XPS spectrum of the nano tetraimine Pd(0) complex with expansion.

that imine groups can suppress the agglomeration of Pd nanoclusters, and enhance the catalytic efficiency of Pd nanoparticles.[35]

Application of the nano tetraimine Pd(0) complex as a catalyst in the Heck–Mizoroki reaction

Initial studies were performed on the Heck coupling reaction of iodobenzene (1.0 mmol) with n-butyl acrylate (1.2 mmol) as a model reaction using the nano tetraimine Pd(0) complex (0.005 g) as the catalyst in water at 90 °C for 5 h. As can be seen in Table 1, from the bases screened, K$_2$CO$_3$ shows the best result, and the corresponding coupling product was obtained in 94% yield (Table 1, entry 11). When the amount of the catalyst was decreased from 0.005 to 0.002 g, the yield of the product was decreased to 34% (Table 1, entry 13). An almost similar yield was achieved when escalating the catalyst amount from 0.005 g to 0.006 g (Table 1, entry 16). The effect of temperature on the activity of the catalyst was also studied by carrying out the model reaction at different temperatures and the best result was obtained at 90 °C (Table 1, entry 11).

Table 1 Optimization of different proportions of the nano tetraimine Pd(0) complex and the effect of the amount of catalyst, solvents, temperature and using different bases upon the reaction of iodobenzene with n-butyl acrylate[a]

Entry	Solvent	Catalyst amount (g)	Bases	Temperature (°C)	Yield[b] (%)
1	DMF	0.005	K$_2$CO$_3$	90	85
2	NMP	0.005	K$_2$CO$_3$	90	80
3	DMSO	0.005	K$_2$CO$_3$	90	68
4	CH$_3$CN	0.005	K$_2$CO$_3$	Reflux	44
5	Toluene	0.005	K$_2$CO$_3$	90	35
6	THF	0.005	K$_2$CO$_3$	Reflux	23
7	EtOH	0.005	K$_2$CO$_3$	Reflux	79
8	EtOH/H$_2$O [3/1 (v/v)]	0.005	K$_2$CO$_3$	90	82
9	EtOH/H$_2$O [2/1 (v/v)]	0.005	K$_2$CO$_3$	90	82
10	EtOH/H$_2$O [1/1 (v/v)]	0.005	K$_2$CO$_3$	90	86
11	H$_2$O	0.005	K$_2$CO$_3$	90	94
12	H$_2$O	None	K$_2$CO$_3$	100	—
13	H$_2$O	0.002	K$_2$CO$_3$	90	34
14	H$_2$O	0.003	K$_2$CO$_3$	90	45
15	H$_2$O	0.004	K$_2$CO$_3$	90	76
16	H$_2$O	0.006	K$_2$CO$_3$	90	93
17	H$_2$O	0.005	None	90	—
18	H$_2$O	0.005	Na$_2$CO$_3$	90	85
19	H$_2$O	0.005	Cs$_2$CO$_3$	90	88
20	H$_2$O	0.005	Et$_3$N	90	41
21	H$_2$O	0.005	NaOAc	90	51
22	H$_2$O	0.005	NaOH	90	62
23	H$_2$O	0.005	KF	90	48
24	H$_2$O	0.005	K$_2$CO$_3$	r.t.	Trace
25	H$_2$O	0.005	K$_2$CO$_3$	80	90
26	H$_2$O	0.005	K$_2$CO$_3$	100	94
27	None	0.005	K$_2$CO$_3$	90	73

[a] Reactions were run in 3 mL solvent with 1.0 mmol iodobenzene, 1.2 mmol n-butyl acrylate, and 2.0 mmol base for 5 h. [b] Isolated yield.

This reaction was tested under solvent free conditions at 90 °C (Table 1, entry 27) and observed 73% yield. Furthermore, we also screened the use of different organic solvents such as DMF, NMP, DMSO, CH$_3$CN, EtOH, EtOH/H$_2$O, THF and toluene at 90 °C (Table 1, entries 1–11) and excellent yield of the product was observed in H$_2$O (Table 1, entry 11).

In order to verify the higher activity of the catalyst, its activity towards other substrates with the variation of different substituents was examined. The optimized reaction conditions were applied in the Heck–Mizoroki cross-coupling reaction of different types of aryl halides under conventional heating at 90 °C.

As shown in Table 2, a range of aryl iodides and bromides reacted with olefins to give the desired products in high yields. As expected, the reaction of aryl iodides bearing electron donating groups went to completion in longer reaction times (Table 2, entries 3–5 and 17–19) than those with electron-withdrawing groups (Table 2, entries 2 and 16). The coupling reaction of *n*-butyl acrylate and styrene with both electron-donating and electron withdrawing substituted aryl bromides afforded the desired products in high yields (Table 2, entries 7–14, 20 & 25). In general, the coupling reactions with acrylates as the olefin were faster than styrene.

Heterogeneous test and recyclability

The possibility of recycling the catalyst is very important and makes it useful for commercial applications. Thus, we investigated the recovery and reusability of the catalyst using iodobenzene and *n*-butyl acrylate (Heck–Mizoroki reaction) (Fig. 5) as model substrates. Six consecutive cycles of the reaction showed that the catalyst did not lose its activity and could be recycled. To determine the exact Pd species which is responsible for the observed reactions and to measure the extent of Pd leaching after the reactions, we used the hot filtration test.[38] The hot filtration test was performed in order to determine whether the catalyst was acting in a truly heterogeneous manner or whether it is merely a reservoir for the more active soluble form Pd. In a typical experiment, Pd complex (0.4 mol%), iodobenzene (1 mmol), *n*-butyl acrylate (1.2 mmol), K$_2$CO$_3$ (2.0 mmol) and water (3 ml) were taken in a round-bottom flask and stirred at 90 °C. The resulting solution was further heated at 90 °C under the previous conditions. GC analysis of the reaction mixture showed only 41% conversion of iodobenzene after 5 h which is only a 5% increase in the amounts of the produced product. This result clearly shows that the amount of leaching of the catalyst into the reaction mixture should be low and confirms that the catalyst acts heterogeneously in the reaction. In order to obtain more information about the leaching of palladium, the reaction of iodobenzene with *n*-butyl acrylate as a model reaction was studied. After completion of the reactions and the work-up, the amount of leaching was determined by ICP analysis in 8 repeating cycles. Low palladium corruption was observed during this experiment. Analysis of the crude reaction mixture for the first reaction indicates a leaching of 0.21% of the palladium. Residual palladium levels present in the solution for different catalytic runs were also analyzed. This catalytic system shows 4.17% of palladium leaching after 8 runs, which justifies the decrease in the yield after run 7 (Fig. 6).

The amounts of the nano tetraimine Pd leaching for the reactions under the optimized conditions were detected. The Pd content in the reaction medium after each reaction cycle was measured by ICP and details are provided in Fig. 7. The analysis of the reaction mixture by the ICP technique showed that the leaching was negligible.

In order to show the applicability of this nano catalyst for large scale reactions, the reaction of iodobenzene and *n*-butyl acrylate was performed on a 10 mmol scale. The reaction performed very well and the coupled product was obtained in excellent yield. The catalyst was also recycled and reused again.

Theoretical calculations

In order to investigate the preference of cationic and neutral pathways, we have theoretically studied the model Heck reaction between PhI and ethyl acrylate (EA). The use of ethyl acrylate instead of butyl acrylate was due to its lower steric factor which is more suitable for theoretical calculation (Scheme 3). On the basis of our spectrometric study, the structure of the catalyst was shown to be a tetraimine complex of palladium (ML$_2$) as shown in Scheme 2.

Geometry and frequency calculations were performed with the hybrid density functional theory method B3LYP. A previous work[39] has shown that the B3LYP energies are similar to CCSD(T) for CH$_4$ oxidative addition to Pd. All structures were fully optimized in the gas phase with default convergence criteria. Moreover, frequencies were calculated to ensure that there are no imaginary frequencies for minima and only one imaginary frequency for transition states. Zero point energies and thermodynamic functions were calculated at 298.15 K and 1 atm. For light atoms the calculations have been performed with the 6-31G* basis set, while for heavy elements (Pd and I) the SDD basis set has been used to specify effective core potential within the pseudo-potential input. This basis set was found to satisfactorily reproduce experimental properties such as geometrical configurations and vibrational frequencies for a range of molecules. Natural population analysis was also employed to describe the state of charge transfer by the use of the natural bond orbital (NBO)[40] analysis implemented in Gaussian 09.[41]

First let us to have a brief discussion on the electronic properties of tetraimine Pd(0). Fig. 8 shows the optimized structures of the experimentally synthesized tetraimine Pd(0) complex **4′** together with selective structural parameters. It is obvious that the complex has two longer Pd–N bonds with 2.227 Å and two Pd–N bonds with a bond length of 2.195 Å. The calculated NBO charge distributions indicate that the palladium atom carries a positive charge of 0.21e with the natural electron configuration of [core] 5s(0.31) 4d(9.14) 5p(0.32) 5d(0.01) 6d(0.01). On the other hand the negative charge of 0.47e on nitrogen atoms is consistent with the electron configuration of [core] 2s(1.36) 2p(4.10) 3p(0.01). These configurations

Table 2 Heck–Mizoroki coupling of different aryl halides with *n*-butyl acrylate or styrene in the presence of the nano tetraimine Pd(0) complex[a]
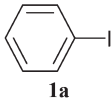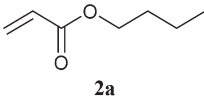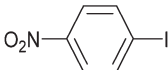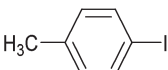

Entry	Aryl halide	Alkene	Product	Time (h)	Yield[b] (%)	TON	TOF[c] (h^{-1})	Ref.
1	1a	2a	3a	1	94	235	235	36
2		2a	3b	0.5	96	240	480	37
3		2a	3c	2	91	227.5	113.75	37
4		2a	3d	2.5	92	230	100	36
5		2a	3e	2	89	222.5	111.25	36
6		2a	3f	1.5	95	237.5	158.33	9
7		2a	3a	3	91	227.5	75.8	37
8		2a	3b	2	93	232.5	116.25	37
9		2a	3g	2	91	227.5	113.75	37
10		2a	3h	2.5	93	232.5	93	9
11		2a	3c	5	89	222.5	44.5	37
12		2a	3d	5	86	215	43	36
13		2a	3i	3	86	215	71.6	9
14		2a	3j	2.5	92	230	92	37
15		2b	3k	2.5	93	232.5	93	9

Table 2 *(Contd.)*
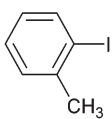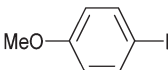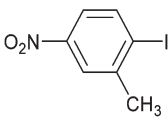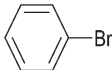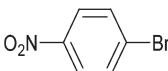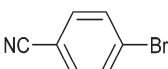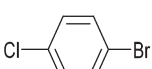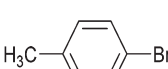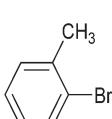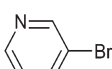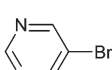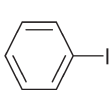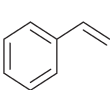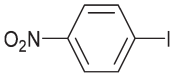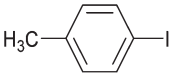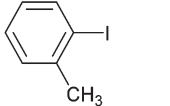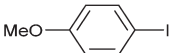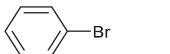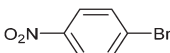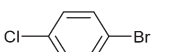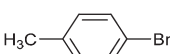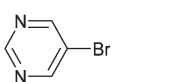
$$R^1 \overset{X}{\underset{}{\bigcirc}} + \overset{}{\diagup} R^2 \xrightarrow[\text{H}_2\text{O, K}_2\text{CO}_3, 90\,^\circ\text{C}]{\text{Pd catalyst (0.4 mol\%)}} R^1 \overset{}{\underset{}{\bigcirc}} \diagup\diagdown R^2$$

3a-r

Entry	Aryl halide	Alkene	Product	Time (h)	Yield[b] (%)	TON	TOF[c] (h⁻¹)	Ref.
16	O₂N—⬡—I	2b	3l	1.5	96	240	160	9
17	H₃C—⬡—I	2b	3m	4	90	225	56.25	9
18	⬡(I)(CH₃)	2b	3n	4	86	215	53.75	37
19	MeO—⬡—I	2b	3o	5	88	220	44	9
20	⬡—Br	2b	3k	5	89	222.5	44.5	36
21	O₂N—⬡—Br	2b	3l	2.5	92	230	92	37
22	NC—⬡—Br	2b	3p	3	90	225	75	37
23	Cl—⬡—Br	2b	3q	3.5	92	230	65.71	36
24	H₃C—⬡—Br	2b	3m	7	84	210	30	36
25	N⬡N—Br	2b	3r	3.5	89	222.5	63.57	37

[a] All reactions were carried out with Ar–X (1.0 mmol), alkene (1.2 mmol), and K_2CO_3 (2.0 mmol) in the presence of the Pd(0) complex (0.005 g) in 3.0 mL of H_2O at 90 °C. [b] Isolated yield. [c] TOF = (mol product per mol cat) h⁻¹.
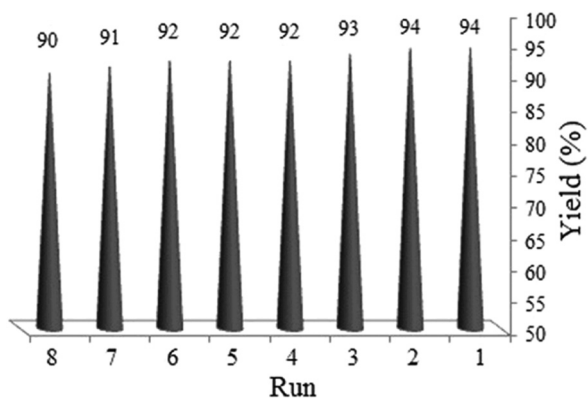
Fig. 5 Recycling of the catalyst for the Heck–Mizoroki reaction. Reaction conditions: iodobenzene or bromobenzene (1 mmol), *n*-butyl acrylate (1.2 mmol), K₂CO₃ (2 mmol), catalyst (0.4 mol%), H₂O (3 mL), 90 °C.

Fig. 6 Leaching Pd in 8 cycles.

clearly indicate the charge transfer from 4d orbital of palladium to the 2p orbital of nitrogen atoms. Fig. 9 gives a pictorial description of the frontier orbitals of a tetraimine Pd(0) complex. As Fig. 9 shows, the highest occupied molecular

Fig. 7 Pd content (mg mol⁻¹) from fresh catalyst to 8 cycles.

orbital (HOMO) is mostly localized on the palladium and nitrogen atoms, while the lowest unoccupied molecular orbital (LUMO) is approximately delocalized along the w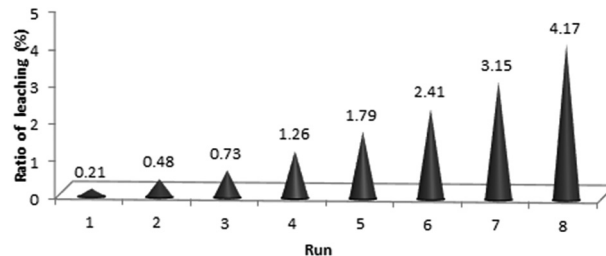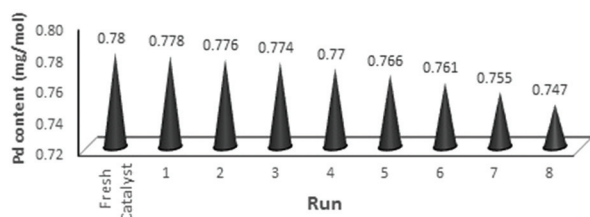hole molecular backbone. The obtained band gap between the HOMO and LUMO orbitals is 3.59 eV at the B3LYP/6-31G*/SDD level of theory.

We have also performed the geometry optimization of complex **4′** in water media. The solute–solvent interaction was modeled using the self-consistent reaction field (SCRF)[42] method. The calculated NBO charge on Pd is 0.04*e* with the natural electron configuration of [core] 5s(0.32) 4d(9.28) 5p(0.35) 5d(0.01) 6d(0.01).

The small positive charge on Pd indicates that the neutral path would be competitive with the cationic path as demonstrated by previous investigations.[30,43]

The catalytic cycle begins with the oxidative addition of PhI to the tetraimine Pd(0) complex. This step is expected to be in conjunction with the dissociation of tetraimine Pd(0) to bisimine Pd. The dissociation has been previously reported in the case of bulky phosphine ligands leading to the belief that monophosphine palladium complexes are more active in the oxidative addition reactions.[44,45] Furthermore, theoretical studies have shown that the barriers calculated for oxidative addition of RX to PdL are significantly smaller when compared to those of RX to PdL$_2$.[46] However, we have theoretically confirmed the dissociation of tetraimine Pd(0) as the optimization of six coordinated Pd did not converge to stable geometry. Therefore, it is suggested that the active species in the oxidative addition is probably bisimine Pd in which the iodide ligand is *cis* with respect to the pyrazole ring. The alternative *trans* isomer is 0.74 kcal mol⁻¹ higher in energy at our level of calculations. After oxidative addition, the next step in the mechanism involves the attack on the palladium center by a C═C bond of the EA to afford a π complex. In the cationic pathway, the dissociation of the Pd–I bond occurs before this step, so the cationic complex **10** is formed. However, alkene EA coordinates to **5** and **10** to form **6** and **11** complexes, respectively. Table 3 presents the Gibbs reaction energies for such processes, and the corresponding free energy profiles are shown in Fig. 10. Moreover, the structures of the stationary points are presented in Fig. 11.

The Gibbs formation energies of complexes **6** and **11** are, respectively, 7.30 and −9.96 kcal mol⁻¹. The large difference is due to the fact that in **10** there is a vacant coordination site whereas in **6** the coordination site is occupied by the iodide.
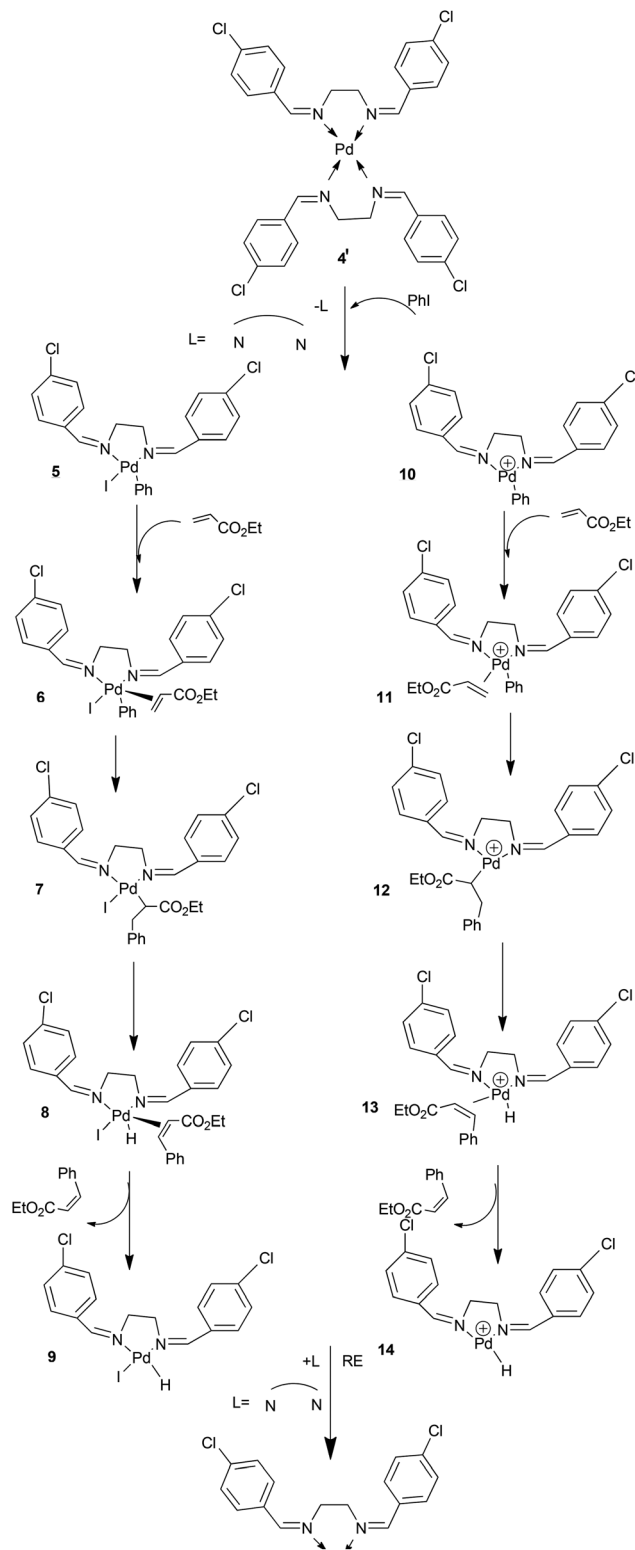
Scheme 3 The neutral (left) and cationic (right) mechanisms for the Heck reaction.

The reaction proceeds with the migratory insertion of the C═C bond into the Pd–Ph moiety to attain complexes 7 and 12 in the neutral and cationic pathways, respectively. This
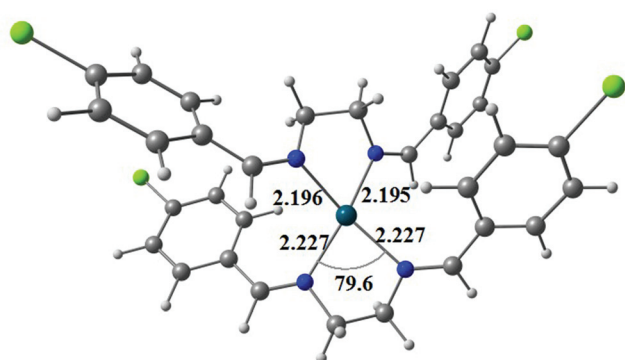
Fig. 8 Optimized structure of the tetraimine Pd (0) complex. Bond angles and bond lengths are given in degree and angstrom, respectively.
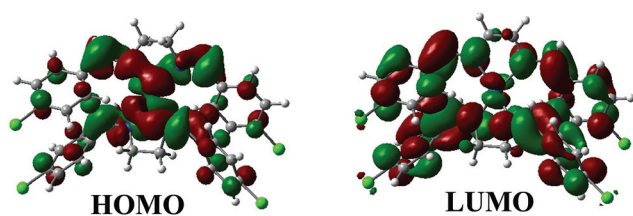
Fig. 9 Spatial distributions of frontier molecular orbitals of the tetraimine Pd(0) complex. The red and green colors stand for electrons and holes, respectively.

Table 3 Gibbs reaction energies for the reaction between PhI and EA in neutral and cationic pathways[a]

	ΔG (kcal mol^{-1})		ΔG (kcal mol^{-1})
5 + EA→**6**	7.30	**10** + EA→**11**	−9.60
6→**7**	−14.93	**11**→**12**	−14.83
7→**8**	10.65	**12**→**13**	33.40
8→**9** + Prod.	−10.67	**13**→**14** + Prod.	−7.92

[a] The calculations have been performed at 298.15 K.

Fig. 10 Gibbs free energy profiles for the competition between cationic and neutral pathways.

Fig. 11 Structures of stationary points corresponding to the neutral and cationic pathways in Scheme 2.

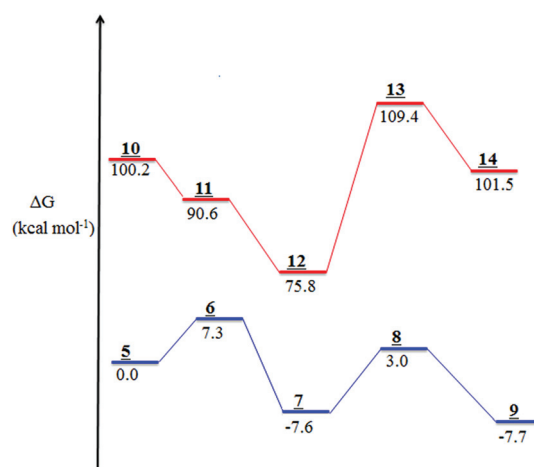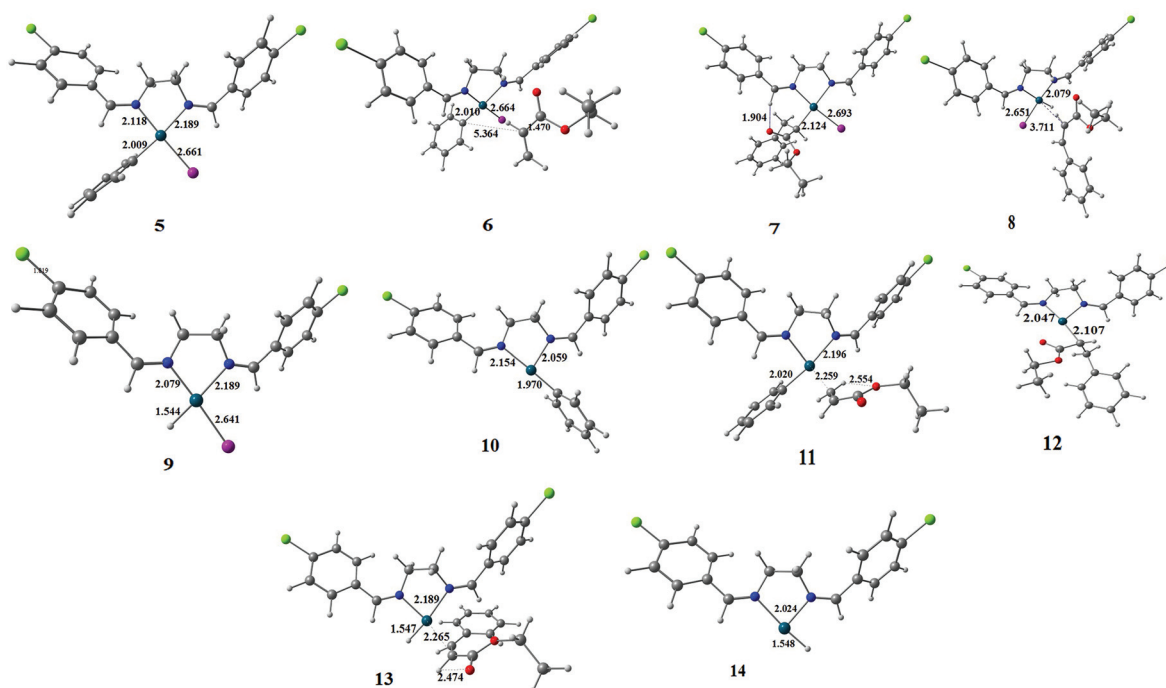process involves the formation of a C–C bond between the phenyl group and the non-substituted carbon atom of the EA ligand. Previous studies show that the formation of the bond involving the substituted carbon atom of the alkene involves a very large energy barrier.[47] In this step there is no notable difference between the neutral and cationic pathways. The calculated Gibbs reaction energy of the neutral path is -14.93 kcal mol^{-1} which is comparable with -14.83 kcal mol^{-1} for the cationic path. The next step is β-hydride elimination to give a new C=C bond in complexes **8** and **13** and to finally form carbonyl product along with the formation of **9** and **12**. The Gibbs reaction energies for the dissociation of **7** to the complex **8** are significantly lower than the dissociation of **12** to complex **13**. The calculated ΔGs are 10.65 and 33.40 kcal mol^{-1}, respectively, for the former and latter reactions. In fact, this step differentiates the neutral *versus* cationic pathways. The final step involves -10.67 and 7.92 kcal mol^{-1} energy to give complexes **9** and **14**. However, despite these differences, the Gibbs free energy profiles for the two neutral and cationic mechanisms do not change sufficiently to suggest the preference of one *versus* the other. The differences in activation barriers are small, and subject to computational uncertainty, the cationic path would be expected to be competitive with the neutral path.

Conclusion

In conclusion, we have developed a novel, practical and economical nano tetraimine Pd(0) complex catalyst system for the cross-coupling reactions. This catalyst demonstrated high catalytic activities in the Heck–Mizoroki reactions for synthesizing some of the alkene derivatives with high yield under mild, and green conditions in a heterogeneous system with short reaction times. Moreover, the catalyst offers notable advantages such as facile recovery from the reaction mixture, easy preparation, and simplicity of handling. All these advantages make this protocol a convenient process for other metal catalyzed reactions. After the reaction, the leaching of palladium into the solution is very low as indicated by ICP. In addition, the catalyst can be readily recovered and reused several times without significant loss of the catalytic activity. The catalytic activity of tetraimine Pd(0) has also been theoretically investigated by comparing the cationic and neutral pathways in a model Heck reaction between PhI and ethyl acrylate. Although the energy barriers of the two paths are different, the Gibbs free energy profiles suggest that the cationic path may be competitive with the neutral path. However, the preference of one pathway to the other depends on several factors such as the polarity of the solvent, the bulkiness of the ligand, and the halide ion.

Acknowledgements

Notes and references

1 P. Baumeister, G. Seifert and H. Steiner (Ciba-Geigy AG), *European Patent*, EP584043, 1994.
2 J. Yang, D. Wang, W. Liu, X. Zhang, F. Bian and W. Yu, *Green Chem.*, 2013, **15**, 3429.
3 N. M. Jenny, M. Mayor and T. R. Eaton, *Eur. J. Org. Chem.*, 2011, 4965–4983.
4 M. B. Goldfinger, K. B. Grawford and T. M. Swager, *J. Am. Chem. Soc.*, 1997, **119**, 4578–4593.
5 A. Balanta, G. Cyril and C. Carmen, *Chem. Soc. Rev.*, 2011, **40**, 4973–4985.
6 M. Oberholzer and C. M. Frech, *Green Chem.*, 2013, **15**, 1678–1686.
7 S. Gao, Y. Huang, M. Cao, T. Liu and R. Cao, *J. Mater. Chem.*, 2011, **21**, 16467.
8 B. Punji, C. Ganesamoorthy and M. S. Balakrishna, *J. Mol. Catal. A: Chem.*, 2006, **259**, 78–83.
9 N. Iranpoor, H. Firouzabadi, S. Motevalli and M. Talebi, *J. Organomet. Chem.*, 2012, **708–709**, 118–124.
10 D. Bourissou, O. Guerret, F. P. Gabbai and G. Bertrand, *Chem. Rev.*, 2000, **100**, 39–92.
11 N. M. Motsoane, I. A. Guzei and J. Darkwa, *Z. Naturforsch., B: Chem. Sci.*, 2007, **62**, 323–330.
12 M. W. Jones, R. M. Adlington, J. E. Baldwin, D. D. Le Pevelen and N. Smiljanic, *Inorg. Chim. Acta*, 2010, **363**, 1097–1101.
13 C. Najera, J. Gil-Moito, S. Karlstrum and L. R. Falvello, *Org. Lett.*, 2003, **5**, 1451–1454.
14 J. C. Xiao, B. Twamley and J. M. Shreeve, *Org. Lett.*, 2004, **6**, 3845–3847.
15 S. Haneda, C. Ueba, K. Eda and M. Hayashi, *Adv. Synth. Catal.*, 2007, **349**, 833–835.
16 W. Chen, C. Xi and Y. Wu, *J. Organomet. Chem.*, 2007, **692**, 4381–4388.
17 S. Iyer, G. M. Kulkarni and C. Ramesh, *Tetrahedron*, 2004, **60**, 2163–2172.
18 T. Mino, Y. Shirae, Y. Sasai, M. Sakamoto and T. Fujita, *J. Org. Chem.*, 2006, **71**, 6834–6839.
19 P. Srinivas, P. R. Likhar, H. Maheswaran, B. Sridhar, K. Ravikumar and M. L. Kantam, *Chem. – Eur. J.*, 2009, **15**, 1578–1581.
20 S. O. Kang, M. A. Hossain and K. Bowman-James, *Coord. Chem. Rev.*, 2006, **250**, 3038–3052.
21 S. O. Kang, R. A. Begum and K. Bowman-James, *Angew. Chem., Int. Ed.*, 2006, **118**, 8048–8061.
22 M. O. Simon and C. J. Li, *Chem. Soc. Rev.*, 2012, **41**, 1415–1427.
23 P. Anastas and N. Eghbali, *Chem. Soc. Rev.*, 2010, **39**, 301.
24 C. C. Tzschucke, C. Markert, W. Bannwarth, S. Roller, A. Hebel and R. Haag, *Angew. Chem., Int. Ed.*, 2002, **41**, 3964–4000.
25 H. D. Velazquezd and F. Verpoort, *Chem. Soc. Rev.*, 2012, **41**, 7032–7060.
26 A. Kamal, V. Srinivasulu, B. N. Seshadri, N. Markandeya, A. Alarifib and N. Shankaraiah, *Green Chem.*, 2012, **14**, 2513.

27 H. V. Schenck, B. Åkermark and M. Svensson, *J. Am. Chem. Soc.*, 2003, **125**, 3503.

28 B. L. Lin, L. Liu, Y. Fu, S. W. Luo, Q. Chen and Q. X. Guo, *Organometallics*, 2004, **23**, 2114.

29 R. J. Deeth, A. Smith and J. M. Brown, *J. Am. Chem. Soc.*, 2004, **126**, 7144.

30 C. Bäcktorp and P. O. Norrby, *Dalton Trans.*, 2011, **40**, 11308.

31 Y. Yang, Y. Zhang, S. Hao, J. Guan, H. Ding, F. Shang, P. Qiu and Q. Kanm, *Appl. Catal., A*, 2010, **381**, 274–281.

32 A. Khalafi-Nezhad and F. Panahi, *Green Chem.*, 2011, **13**, 2408–2415.

33 (*a*) H. Firouzabadi, N. Iranpoor and H. Azadi, *J. Organomet. Chem.*, 2008, **693**, 2469–2472; (*b*) H. Firouzabadi, N. Iranpoor and H. Azadi, *Eur. J. Org. Chem.*, 2007, 2197–2201.

34 J. P. Mathew and M. Srinivasan, *Eur. Polym. J.*, 1995, **31**, 835–839.

35 D. Yi, S. Lee and J. Ying, *Chem. Mater.*, 2006, **18**, 2459–2461.

36 H. Firouzabadia, N. Iranpoora, F. Kazemia and M. Gholinejad, *J. Mol. Catal. A: Chem.*, 2012, **357**, 154–161.

37 H. Firouzabadi, N. Iranpoor and A. Ghaderi, *J. Mol. Catal. A: Chem.*, 2011, **347**, 38–45.

38 E. Mohsen, S. Ali Reza and J. Jaber, *J. Organomet. Chem.*, 2014, **749**, 233–240.

39 G. T. D. Jong, D. P. Geerke, A. Diefenbach and F. M. Bickelhaupt, *Chem. Phys.*, 2005, **313**, 261–270.

40 A. E. Reed, L. A. Curtiss and F. A. Weinhold, *Chem. Rev.*, 1998, **88**, 899–926.

41 M. J. Frisch, G. W. Trucks, H. B. Schlegel, G. E. Scuseria, M. A. Robb, J. R. Cheeseman, G. Scalmani, V. Barone, B. Mennucci, G. A. Petersson, H. Nakatsuji, M. Caricato, X. Li, H. P. Hratchian, A. F. Izmaylov, J. Bloino, G. Zheng, J. L. Sonnenberg, M. Hada, M. Ehara, K. Toyota, R. Fukuda, J. Hasegawa, M. Ishida, T. Nakajima, Y. Honda, O. Kitao, H. Nakai, T. Vreven, J. A. Montgomery Jr., J. E. Peralta, F. Ogliaro, M. Bearpark, J. J. Heyd, E. Brothers, K. N. Kudin, V. N. Staroverov, R. Kobayashi, J. Normand, K. Raghavachari, A. Rendell, J. C. Burant, S. S. Iyengar, J. Tomasi, M. Cossi, N. Rega, J. M. Millam, M. Klene, J. E. Knox, J. B. Cross, V. Bakken, C. Adamo, J. Jaramillo, R. Gomperts, R. E. Stratmann, O. Yazyev, A. J. Austin, R. Cammi, C. Pomelli, J. W. Ochterski, R. L. Martin, K. Morokuma, V. G. Zakrzewski, G. A. Voth, P. Salvador, J. J. Dannenberg, S. Dapprich, A. D. Daniels, O. Farkas, J. B. Foresman, J. V. Ortiz, J. Cioslowski and D. J. Fox, *GAUSSIAN 09 (Revision A.02)*, Gaussian, Inc., Wallingford, CT, 2009.

42 M. W. Wong, M. J. Frisch and K. B. Wiberg, *J. Am. Chem. Soc.*, 1991, **113**, 4776.

43 P. Surawatanawong, Y. Fan and M. B. Hall, *J. Organomet. Chem.*, 2008, **693**, 1552–1563.

44 U. Christmann and R. Vilar, *Angew. Chem., Int. Ed.*, 2005, **44**, 366.

45 J. P. Knowles and A. Whiting, *Org. Biomol. Chem.*, 2007, **5**, 31–44.

46 M. Ahlquist and P. O. Norrby, *Organometallics*, 2007, **26**, 550.

47 H. V. Schenck, S. Strömberg, K. Zetterberg, M. Ludwig, B. Akermark and M. Svensson, *Organometallics*, 2001, **20**, 2813.